Biorheology 00 (20xx) 1–14
DOI 10.3233/BIR-14014
IOS Press

Influence of mycosporine-like amino acids and gadusol on the rheology and Raman spectroscopy of polymer gels

Maira Gaspar Tosato [a], Dalila E. Orallo [b], M. Sandra Churio [b], Airton A. Martin [c], Claudio A. Telléz Soto [c] and Lelia E. Dicelio [a,*]

[a] *Universidad de Buenos Aires, INQUIMAE, Buenos Aires, Argentina*
[b] *Facultad de Ciencias Exactas, Universidad Nacional de Mar del Plata, Mar del Plata, Argentina*
[c] *Laboratório de Espectroscopia Vibracional Biomédica, Universidade do Vale do Paraíba, Sao José dos Campos, Brasil*

Received 8 April 2014
Accepted in revised form 3 October 2014

Abstract.
BACKGROUND: The amphiphilic nature of polymers allows them to be widely incorporated as carriers in different pharmaceutical applications since they are able to work as vehicles for hydro- or lipo-soluble actives.
OBJECTIVE: The aim of this study was to determine the rheological behavior and vibrational spectral variations of two hydrophilic gels prepared with Poloxamer 407 (PO) or Pluronic F-127 (PL) with the addition of the actives mycosporine-like amino acids and gadusol.
METHODS: The structures of these polymers in two different concentrations (20% w/w and 27% w/w) were characterized by rheological studies and Raman spectroscopy.
RESULTS: Gels prepared with higher polymer concentration showed larger G' (storage modulus) values. The C–C stretch and the CH_2 rocking predominated in the gels containing PL (20% w/w) and this correlated with a less viscous behavior. The mixture of the actives induced higher contributions of Raman peaks related to *trans* conformation of the C–C bonds located in hydrophilic polymer blocks, whereas the same peaks decreased in the sample containing only gadusol.
CONCLUSIONS: Larger tensile strength and elastic component were observed upon increasing polymer concentration, thus evidencing polymer–polymer and/or polymer–polymer–actives interactions. The presence of the actives affected the mechanical properties of the polymer gels. Gadusol particularly seems to alter the conformation of the polymer chains by favoring *gauche* orientations, in parallel with rising viscoelastic parameters. More stretched arrangements of the polymer are probably induced in the presence of larger concentration of actives, due to specific interactions with their hydrophilic groups.

Keywords: Triblock copolymers, viscoelastic, mycosporine-like amino acids, gadusol

1. Introduction

Cosmetics and bases for dermatological products are currently prepared by using hydrophilic gels. These gels show good application and spread ability, providing feeling of freshness and low oiliness. Amphiphilic polymers can work as vehicles for both hydro- or lipo-soluble actives, thus are widely used

*Address for correspondence: Lelia E. Dicelio, Universidad de Buenos Aires, INQUIMAE, Buenos Aires, Argentina. Tel.: +54 1145763378 (extension line 230); E-mail: led@qi.fcen.uba.ar.

as carriers in different pharmaceutical applications [1–3]. The properties of skin care products depend on the type of polymer used as this may influence the set of interactions between skins, drugs and base.

Surfactant gels (also called hydrogels) are composed of block copolymers that may exhibit ionic or nonionic characters. Nonionic gels are stable in a wide range of pH values, whereas ionic ones are only stable at neutral pH. Pluronic F-127 (PL) and Poloxamer 407 (PO) are two main polymers used in the preparation of hydrogels. These polymers are characterized as triblock copolymers forming thermoreversible gels that modify the bonds responsible for the network structure. This feature makes them suitable to work as vehicles in different routes of administration, for example in controlled dermal and transdermal drug release systems. In addition, they are able to increase the residence time of drugs in the *stratum corneum* and epidermis [4,5]. Triblock copolymers consisting of a polyoxypropylene (PPO, hydrophobic) in the middle and one polyoxyethylene (PEO, hydrophilic) on each side present the general formulation $HO(C_2H_4O)_x(C_3H_6O)_y(C_2H_4O)_zH$. PO has an average molecular weight between 9840 and 14,600 Da, at a ratio of 71.5 to 74.9% ethylene oxide, whereas PL is composed of 70% ethylene oxide with an average molecular weight of 13,000 Da [6,7]. Aqueous solutions of these polymers show good solubilizing capacity, low toxicity, and biocompatibility, and undergo reverse thermal gelation, summing up important properties for the formation of drug delivery systems [8–10].

In the last decades, natural products, such as algae, have been increasingly used in numerous commercial applications and as therapeutic drugs. Compounds extracted from macroalgae show a broad range of biological properties, such as antioxidant, antitumoral and sunscreening capacities that support applications in the cosmetic, food and pharmaceutical industries [11–13]. Mycosporine-like amino acids (MAA), such as shinorine and porphyra-334, and gadusols (Gad), are isolated from red algae and fish roes, respectively. MAA and Gad show photoprotective properties and antioxidant activity, suggesting a promising use in the prevention and therapeutic treatment of skin diseases related to free radicals and UV radiation [11,14].

Rheological investigation indicates material properties in connection to the manufacture, storage and topical application of the products to perform their functions properly. Rheology allows the description of systems containing Newtonian and non-Newtonian fluids by specifying the deformation of the materials under tension. Deformation assesses the stability of the gels and evaluates the effects of adding actives in the solution. In general, non-Newtonian fluids are composed of asymmetric particles like most cosmetic and pharmaceutical products [15,16].

Raman spectroscopy is one of the most powerful techniques to provide not only macroscopic but also microscopic information on the vibrational modes, structure and dynamics of whole molecules and their various functional groups. The Raman spectra of PEO–PPO–PEO triblock copolymers with low molecular weight are very sensitive to structural and conformational changes [17,18].

The aim of this study was to determine the rheological behavior and vibrational spectral variations of two hydrophilic gels prepared by using PO and PL with final concentrations of 20% p/p and 27% p/p, respectively. The rheology and the Raman spectroscopy of the gels with the addition of the actives MAA (0.005% w/v), Gad (0.005% w/v) and the mixture of both were also evaluated.

2. Material and methods

2.1. Materials

PO and PL were purchased from Sigma-Aldrich (Argentina). Ultrapure water from a Milli-Q Water system was used. Three different solutions containing MAA, Gad or MAA + Gad, respectively, in water

were prepared. The proportion of actives in these solutions was adjusted so that the final concentration in the polymer gels was 0.005% w/v.

2.2. MAA and Gad extraction

The MAA shinorine and porphyra-334 were isolated from the red macroalgae *Porphyra leucosticta* as previously described [19]. The samples were collected from the coast of Mar del Plata (Buenos Aires, Argentina) and stored at −20°C until extraction with 50% ethanol: water mixtures. Basically, the extract was concentrated and afterwards treated with methanol by a sequence of evaporation, suspension and centrifugation steps. Then, a concentrated water solution of the solid obtained was eluted with 50% methanol: water from an activated charcoal column. The fractions showing maximal absorbance at 334 nm were collected, eluted with water from an ion exchange resin (Dowex 50W-X8) and finally concentrated in a rotary evaporator. High Performance Liquid Chromatography (HPLC) analysis of the purified extract with an ODS (C18) column and a 0.02% v/v acetic acid in water mobile phase confirmed the presence of shinorine and porphyra-334 in a concentration ratio of *ca* 1:4 [20].

Gadusol was obtained from mature female gonads from the Argentine sand perch (*Pseudopercis semifasciata*). Then, 800-g samples of the gonad content (roes devoid of pelt) were treated according to the procedure described by Plack et al. [21] with minor modifications. Briefly, the unfrozen samples were homogenized in ethanol and kept overnight at low temperature. The suspension was centrifuged and after several cycles of filtering and new extraction with ethanol: water mixtures, the filtrates were combined and concentrated in a rotary evaporator under reduced pressure. The solution was successively washed with ethanol, chloroform and water lots. The resultant aqueous phase was concentrated and treated by ion-exchange chromatography on a Dowex 50W-X (8–400, H^+ form) resin. The fractions containing gadusol were recognized by absorption in the range of 260–300 nm and the reversible shift of the maximum from 268 to 296 nm on going from acid to neutral pH [21,22]. The identification of gadusol was confirmed by HPLC analysis with standard samples [23].

2.3. Preparation of the gels

The gels formed with the solid polymers PO and PL were prepared by the cold method described by Schmolka [24]. Appropriate amounts of PO and PL were weighed to obtain 20% w/w and 27% w/w concentrations of each polymer. In each case, the solids were slowly dissolved in cold Milli-Q water (4–5°C) by gentle mixing for 2–3 min. The solutions were then frozen and kept overnight at 4°C to form a macroscopically homogeneous and transparent solution. Then, aqueous solutions of MAA, Gad or MAA + Gad were respectively added to the cold polymer solutions. The set of concentrations of PO, PL, MAA, Gad and MAA + Gad is summarized in Table 1. To achieve better dissolution of the active in the polymer base, the vials were kept in the refrigerator for 12 h, before the rheological measurements were taken. The pH was determined 48 h after preparation of the gels by using test strips (pH-Fix 0-14, Macherey-Nagel, GmbH & Co.). Gels without actives were used as controls.

2.4. Rheological properties of the gel formulations

The viscoelastic and gelation temperature properties of PO and PL with different actives were evaluated using an Anton Paar Physica MCR 301 rheometer (INTEMA, Mar del Plata, Argentina). The samples were kept refrigerated and taken previously to the data acquisition. A volume of 500 µl of each sample was placed between the parallel sensor plates with 1 mm thickness. The fluids were maintained enclosed in a vacuum system during the measurement as a function of temperature.

Table 1
Gel formulations in the absence of actives (control) and with MAA, Gad and MAA + Gad incorporation

Samples	Gel formulations	Composition			pH
		Concentration (% w/w)	Polymer	Active* (µl)	
1	MPO20	20	Poloxamer 407	350 MAA	7.0
5	GPO20			250 Gad	6.5
9	MGPO20			350 MAA + 250 Gad	7.0
13	PO20			–	7.0
3	MPO27	27	Poloxamer 407	350 MAA	7.0
7	GPO27			250 Gad	6.5
11	MGPO27			350 MAA + 250 Gad	7.0
15	PO27			–	6.5
2	MPL20	20	Pluronic F-127	350 MAA	6.5
6	GPL20			250 Gad	6.0
10	MGPL20			350 MAA + 250 Gad	6.0
14	PL20			–	6.0
4	MPL27	27	Pluronic F-127	350 MAA	6.5
8	GPL27			250 Gad	6.0
12	MGPL27			350 MAA + 250 Gad	6.5
16	PL27			–	6.5

*All the actives were incorporated as aqueous solutions into the gels.

2.4.1. Viscoelastic properties

The low strain amplitude of all the gels was analyzed to determine the viscoelastic region by scanning the stress between 0 and 10^3 Pa. The effect of the temperature (0–40°C) on the apparent viscosity was studied with a constant frequency of 1 Hz (data not shown). A second experiment was performed at different frequencies (0–5 Hz) by maintaining the plate's temperature at 21°C with a digital thermostat. Storage modulus (G') and loss modulus (G'') as a function of the frequency were applied in the material. The small amplitude frequency tests provided information on the linear viscoelastic behavior of the materials through the determination of the complex shear modulus, G^* (Eq. (1)):

$$G^*(\omega) = \sqrt{G'(\omega)^2 + \mathrm{i}G''(\omega)^2}, \tag{1}$$

where ω is the angular frequency, i is the imaginary unit of the complex number and η^* is the complex viscosity defined as in Eq. (2)

$$\eta^*(\omega) = G^*(\omega)/\omega. \tag{2}$$

Thus, $G'(\omega)$ represents the elastic energy component and $G''(\omega)$ the viscous dissipation of the mechanical energy. The mechanical spectrum of $G'(\omega)$ and $G''(\omega)$ yields the quantitative rheological information.

2.4.2. Gelation temperature

Gelation temperature (T_{gel}) is defined as the temperature at which the polymer in the solution becomes a gel. The gelation point was determined at different temperatures between 5 and 40°C, with a heating rate of 2°C min^{-1} and an oscillation frequency of 1 Hz. All samples were placed on the plate at 5°C,

to avoid passing to the gel state. The transition temperature was determined with the η^* value increases sharply to a maximum characterizing the gel state.

2.5. Raman spectroscopy of the gel formulations

The Raman spectra of the gels (Table 1) were measured using a Raman Rivers Diagnostics model 3510 SCA spectrometer. The spectra in the region 400–1800 cm^{-1} were obtained using a 785 nm laser and 25 mW on the sample. The integration time was 10 s with 1 accumulation. Two independent mathematical methods were applied to extract the hidden structural information from the spectra: second derivatives to gain more insight into the overlapping structures and deconvolution of the peaks. The wavenumbers and intensities of the bands in the different regions were obtained from the deconvoluted spectra for the 20% w/w polymers using Gaussian functions. Thus, we compared the information related to the conformational transitions of the different gels. Raman spectra were pre-processed using baseline correction and smoothing functions.

3. Results and discussion

3.1. Rheology

The 20 and 27% w/w aqueous solutions of both polymers explored in this work were liquid at the refrigerator's temperature and decreased their "fluidity" while kept at room temperature, thus becoming a gel-type solution. The gel, in this case, is defined as a polymer network which exhibits no flow when in the steady-state. The dynamic rheology demonstrated the change from liquid to gel for both concentrations. Besides, the pH of all the samples yielded values in the range from 6.0 to 7.0.

The mechanic spectra of the samples, with and without the presence of the actives, are shown in Fig. 1. The dynamic rheology behavior for each sample yields the system's elasticity and viscosity parameters, G' and G'', respectively. It can be seen that the G' and G'' values were higher for low frequency values and that they decreased slowly with increasing frequency, showing that, initially, the difference between these parameters was greater in most of the gels. When increasing the frequency, the elasticity and viscosity values presented the same behavior, indicating the phase change of the system. All measurements were taken at a constant temperature of 21°C. As expected, in all samples and independently of the active, an increase in the concentration of the polymers resulted in an increase in G' and G'' values. However, comparison of the gels at 27% concentration for both polymers indicated a difference between the own storage and loss values, in which G' resulted higher than G'', except for the pure gels. G' has been correlated with the number of intermolecular cross-links in a network [25].

The gelation points were determined by scanning the temperature of the solutions between 5 and 40°C. Figure 2 shows the complex viscosity as a function of temperature for the samples tested at a frequency of 1 Hz. Smaller values of the thermal gelation point were observed in gels with the highest polymer concentration (27% w/w). Both systems share similar temperature patterns. Complex viscosity increased gently during heating until the gelation temperature (T_{gel}) was reached and then showed an abrupt increase in the viscosity in all the cases. Independently of the active, samples at 20% w/w in PO or PL exhibited variations in the T_{gel} values around 3 and 4°C, respectively. The lowest T_{gel} were obtained in gels without actives, for instance: T_{gel} for 20% PL and 20% PO was 23°C and 24°C, respectively. However, samples with a polymer concentration of 27% w/w exhibited similar T_{gel} values and reached the saturation quickly. Higher complex viscosities indicate a more robust network formed by heating.

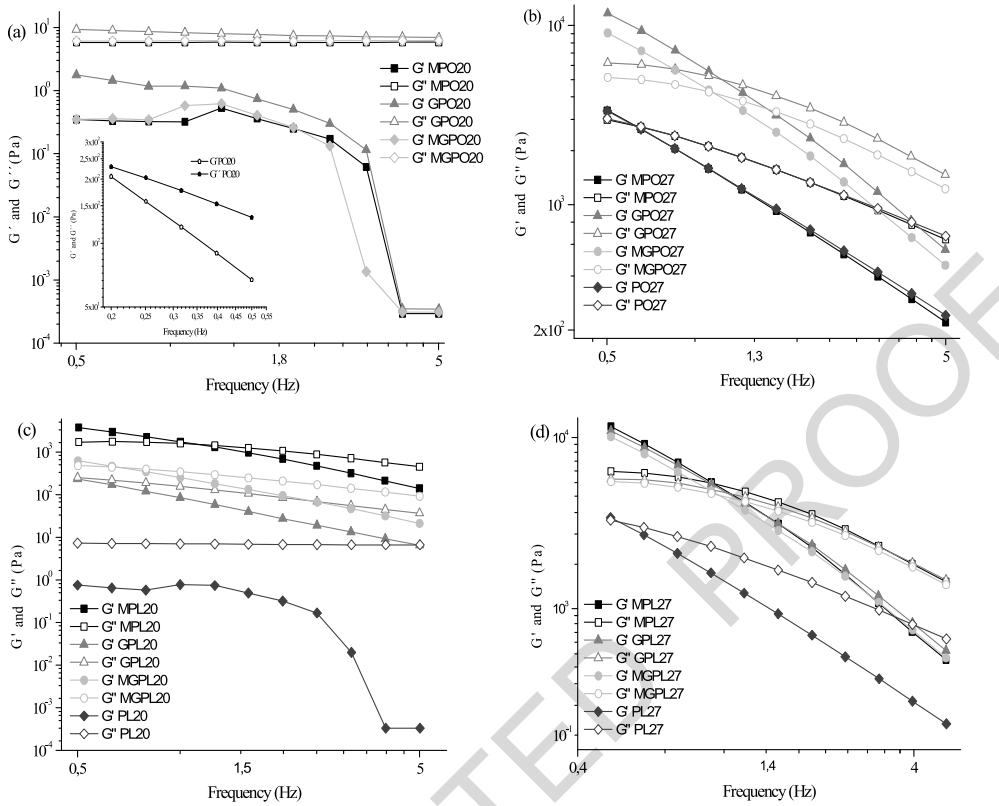

Fig. 1. Frequency dependence of the storage modulus (G') and loss modulus (G''), at different PL (c) and (d) and PO (a) and (b) concentrations and in the presence of the actives. The inset represents the mechanical spectrum of GPO20 control gels.

It is also clear from Fig. 2 that the gel temperature shifts to lower values for higher concentrations of polymers.

3.2. Raman spectroscopy

The results showed that the presence of MAA or Gad in the polymer gels affected the mechanical aspect of the systems. The macroscopic characteristics of the materials are intrinsically linked to their microscopic properties and molecular arrangements. For this reason, Raman spectroscopy is one of the few techniques that can be applied to assess the structural characterization of the hydrocarbon chains with different actives [26,27].

All spectra represented the average of two measurements and the main spectral variations were detected in the following regions: (1) 750–980 cm^{-1}, (2) 990–1200 cm^{-1}, (3) 1210–1380 cm^{-1} and (4) 1380–1500 cm^{-1}. Figure 3(a) shows the Raman spectra of different gel samples. The band centered at 577 cm^{-1} was assigned to the angular deformation of O–C–C and C–O–C bending. These modes are in the limit between the PEO and PPO groups of the polymer molecule. An important band centered at about 851 cm^{-1} corresponds to the CH_2 and C–CH_3 rocking. They are linked to the terminal (PEO) and the central (PPO) groups of the polymer molecule, respectively. The 915–940 cm^{-1} region corresponds to the vibrational mode of CH_2 rocking and C–C, C–O stretching. The 1040–1140 cm^{-1} region represents the C–C, C–O and C–O–C stretching, corresponding to the C–O and O–C oscilla-

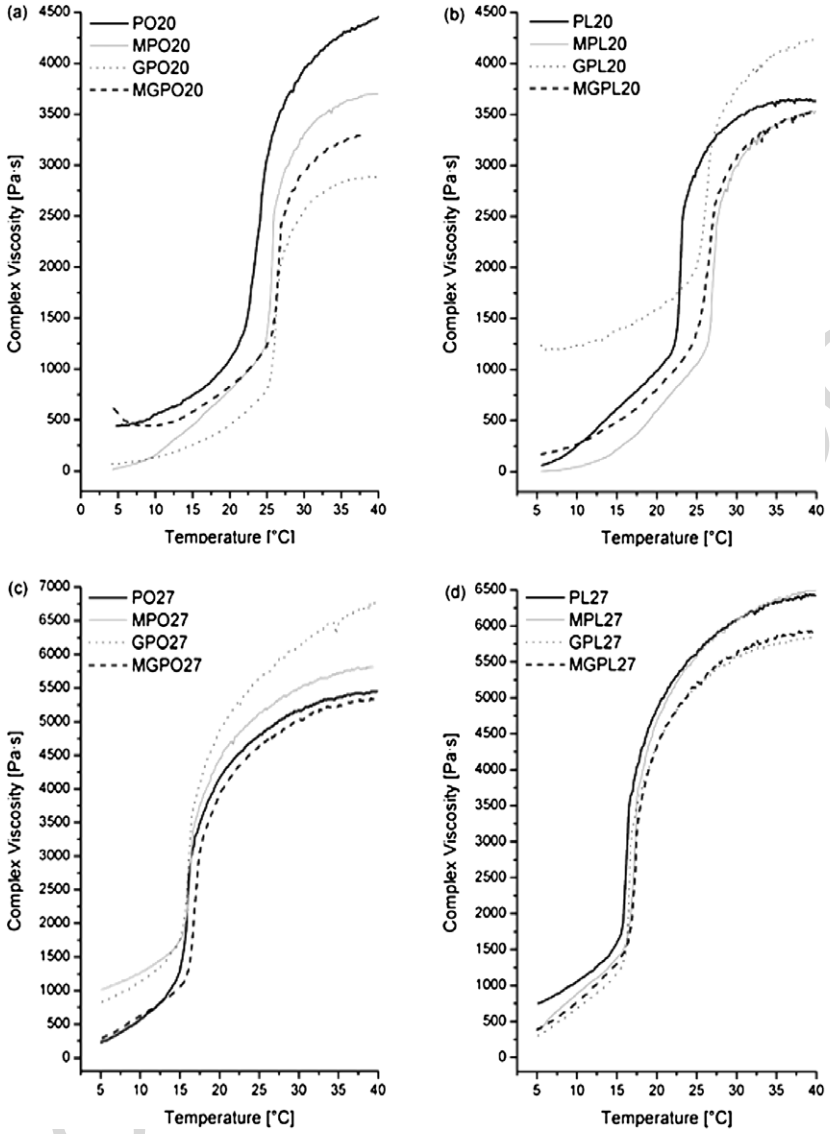

Fig. 2. Complex viscosity at different PO (a) and (b) and PL (c) and (d) concentrations and in the presence of the actives as a function of the temperature.

tor stretching as well as to the C–C skeletal stretch transconformation. The 1240–1285 cm^{-1} region was assigned to the CH_2 twist (angular deformation) and the 1290–1350 cm^{-1} range was attributed to the CH_2 and CH_3 groups with wagging modes [28]. The 1450–1475 cm^{-1} region was assigned to the CH_2 deformation and scissoring modes [17,29–31]. Figure 3(b) shows the characteristic peaks of the Raman spectra for aqueous solutions of MAA and Gad. The MAA solution presents the following principal peaks: 1435 cm^{-1} assigned to the vibrational mode δ(C=CH), indicating the symmetric vibrational stretching of the ring, C–C and C–H stretching modes and/or CH_2 deformations; 1491 cm^{-1} was assigned to the C–N–H bending where the C–N stretching vibration is coupled with the in-plane C–H bending. The characteristic peaks of Gad solutions were: the 881 cm^{-1} band, which corresponds

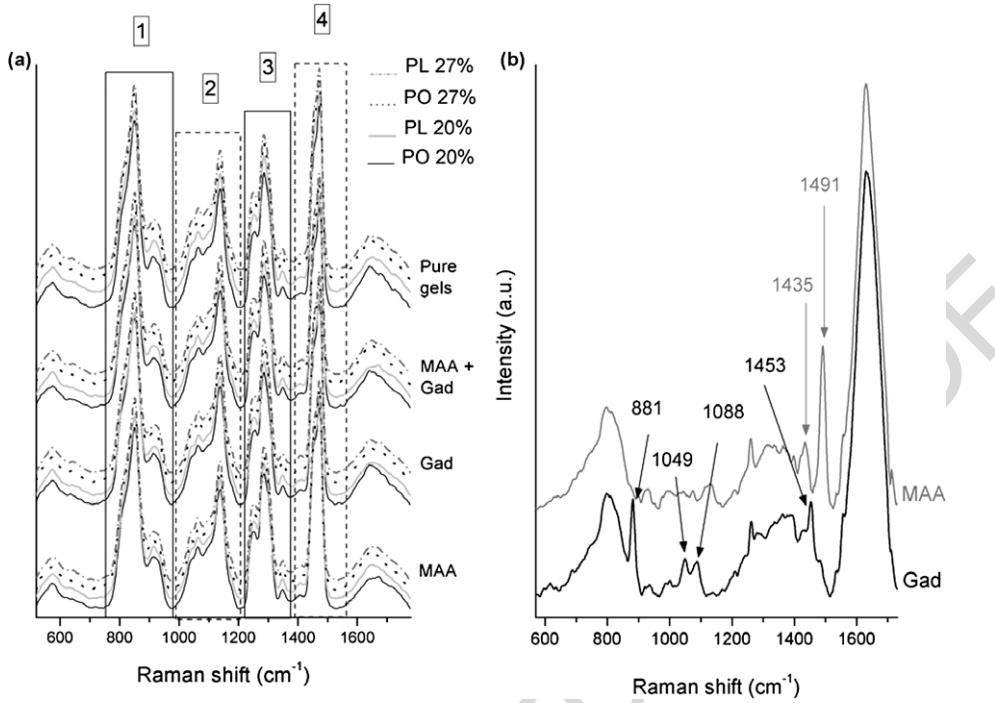

Fig. 3. (a) Comparison of the original Raman spectra for all samples divided in groups: pure gels, gel with mycosporine-like amino acids (MAA), gel with gadusol (Gad) and gel with the mixture MAA + Gad. Four regions are distinguished for the deconvolution analysis: (1) 750–980 cm^{-1}, (2) 990–1200 cm^{-1}, (3) 1210–1380 cm^{-1} and (4) 1380–1500 cm^{-1}; (b) Raman spectra of Gad and MAA in aqueous solutions.

to the a C–C stretching and/or δ(C–C–C); 1049 cm^{-1}, which represents the ν(C–O) enolic and/or C–C stretching; 1088 cm^{-1}, assigned to ν(C–O) enolic and/or C–C skeletal stretch, and the 1453 cm^{-1} band, which corresponds to the CH_3 bending and/or CH_2 bending [26,31–33].

No significant spectral changes were observed in the vibrational spectra of the 16 samples analyzed (Fig. 3(a)). For this reason, the deconvolution method was applied in four different spectral regions described in Fig. 3(a). The spectra of the 20% w/w concentration polymers were analyzed.

The spectra shown in Fig. 3(b) correspond to aqueous solutions of 4.3×10^{-3} M MAA and 9×10^{-3} M Gad, respectively. The second derivative of the Raman spectra for these samples confirmed the differences between the gel structures investigated by verifying the occurrence of overlapping bands. This information was used to perform the band deconvolution analysis of the Raman spectra (Fig. 4(a)–(h)). Table 2 shows the peaks observed and the assignments proposed, related to the conformational changes due to the addition of the active molecules (MAA, Gad and the mixture).

Table 2 summarizes as well the Raman frequencies observed for the control gels with 20% w/w concentration of PO or PL for comparison with the band frequencies of the gels with actives. The table also includes the main peaks, bands and their corresponding assignments [17,29–31,34–36].

For all the gels, eight peaks were observed within the spectral regions analyzed: 850, 1065, 1255, 1282, 1300, 1410, 1454 and 1474 cm^{-1}. The area of the band near 850 cm^{-1} in the gels containing PL was larger than that of the PO gels. In this region, the C–C stretch and the CH_2 rocking predominated. Considering the temperature range of the Raman measurements (15–20°C), this result may be related with the less viscous behavior for PL indicated in Fig. 2. The 20% w/w PO gels increased viscosity at

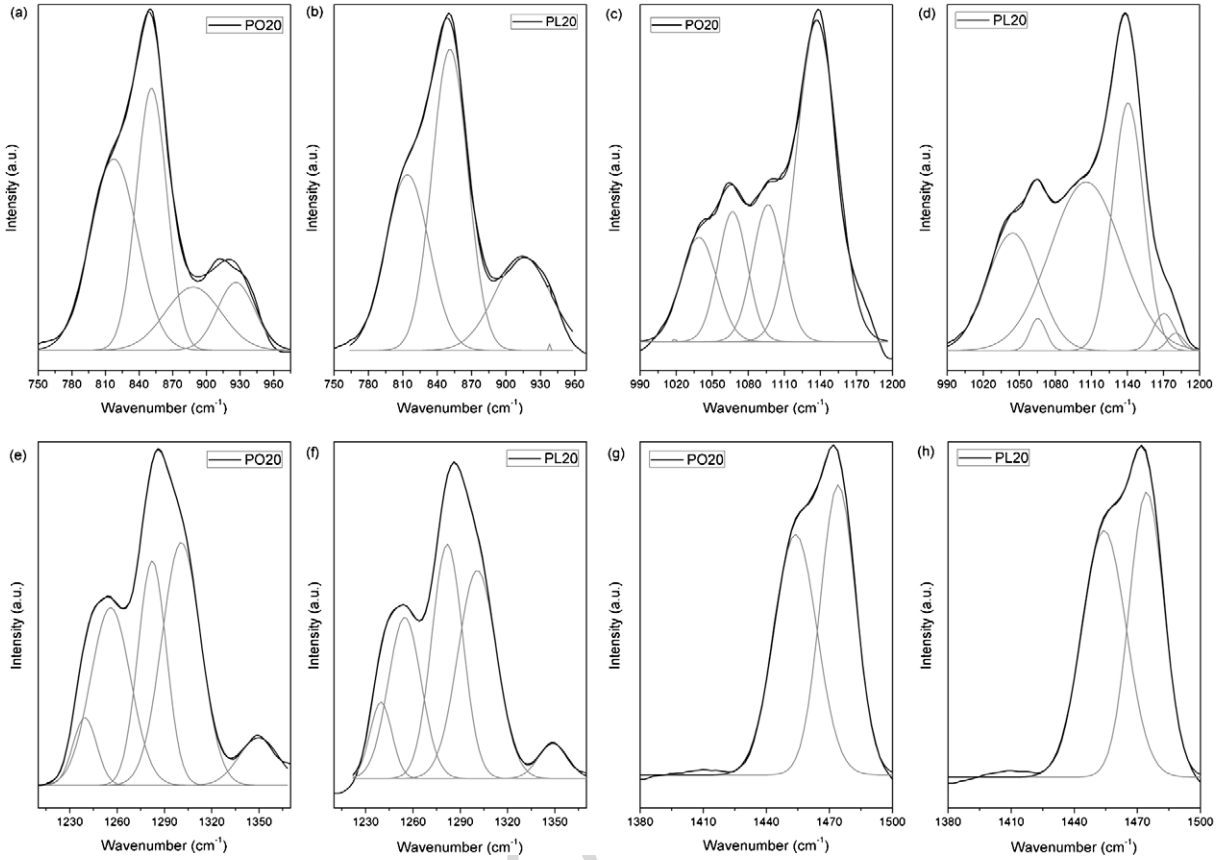

Fig. 4. Curve fitting of Raman spectra of control gels in the frequency ranges (a) and (b): 750–980 cm^{-1}, (c) and (d): 990–1200 cm^{-1}, (e) and (f): 1210–1380 cm^{-1} and (g) and (h): 1380–1500 cm^{-1}. The black and gray lines represent the experimental and calculated spectra, respectively. The signals along these spectral regions were normalized to calculate band areas.

lower temperature when compared with 20% w/w PL gels. In the C–C stretching region, the area of the 1065 cm^{-1} band for the PO gel was 20% larger than for the PL gel corroborated by the values of G' and G'' (Fig. 1) suggesting network formation in the PL gels. The GPO20 sample yielded the lowest area for the bands at 1065 and 1138 cm^{-1}, which are related respectively to the symmetric and the asymmetric *trans* bonds in the C–C backbone. The band near 1088 cm^{-1} due to the skeletal C–C stretching mode of *gauche* segments in the hydrophilic groups (PEO) occurred only in the GPO20 sample.

Differences between the band area values of control gels and gels with actives were found at 1255, 1282, 1300 and 1350 cm^{-1}, and were assigned to the CH_2 twist, $\delta(CH_2)$ of PEO and $\delta(CH_3)_{sym}$, respectively. The sample containing Gad and PO (GPO20) presented a larger area value in 1252 cm^{-1} and a lower wavenumber (shifted up to 4 cm^{-1} compared with other gels) while in 1282 cm^{-1} it showed the lowest value in comparison to the other gels. This result may be due to a more fluid and disordered behavior. The contribution of the CH_2 twist (1300 cm^{-1}) was more intense for MPO20 and MGPL20. The mode corresponding to the symmetric deformation of CH_3 (1350 cm^{-1}) presented a larger area for GPO20 and was absent for the MPO20 sample. In the case of the band at 1410 cm^{-1}, all the samples containing PL yielded a larger area and intensity value. This vibrational mode is related to δ(OH) and $\nu(COO^-)$ and shifts about 4 cm^{-1} for the samples containing PO and 3 cm^{-1} for the samples con-

Table 2
Raman peaks observed and their vibrational assignments for eight different samples

Wavenumber (cm^{-1})								Assignment
PO20	MPO20	GPO20	MGPO20	PL20	MPL20	GPL20	MGPL20	
		813	815	814	815	811		$r(CH_2)$, ν(C–C), ν(C–CH)
817	818						817	
						830		
			833		835			
851	851	850	852	851	851	850	851	
			873					CH_3 rocking, δ(CCC)
888	887		884				892	
		913	912	914	915			
926	927					925	928	ν(C–O), $r(CH_2)$
			937	937				
1019								
1038	1039		1039					$\nu(C–C)_{sym}$, $\nu(CH_3–C)$
	1045	1050		1044	1047	1045	1048	
1067	1062	1065	1068	1065	1065	1067	1064	
		1088						
1096			1098					$\nu(O–CH_2)$
	1110	1110		1105	1102	1102	1106	$r(CH_2)$, $\nu(C–C)_{asym}$ in plane or ν(C–O)
1137		1138	1137		1139			
	1140	1140		1140		1140	1140	
	1174	1174		1170	1172	1175	1174	$r(CH_2)$ in oxyethylene (PEO), (CH) bending
				1180				
			1226					CH_2 twist (PEO), $\delta(CH_2)$
1240	1240		1240	1240	1240	1240	1240	
1255	1255	1252	1256	1254	1255	1255	1254	
1282	1281	1282	1281	1282	1282	1282	1281	
1300	1299	1300	1299	1300	1301	1301	1299	
	1340							$\delta(CH_2)$ wagging, $\delta(CH_3)_{sym}$
1350		1351	1350	1349	1349	1350	1350	
1408	1407	1410	1411	1410	1409	1410	1407	δ(OH), $\nu(COO^-)$
1454	1454	1454	1454	1454	1455	1454	1454	CH_2 symmetric bending, $\delta(CH_2)$ scissor (PEO)
1474	1474	1474	1474	1474	1475	1474	1474	

Notes: δ – deformation; ν – stretching; r – rocking; OE – oxyethylene; sym – symmetric; asym – asymmetric.

taining PL. The CH_2 symmetric bending and $\delta(CH_2)$ scissor region showed two peaks near 1454 and 1474 cm^{-1}. In the PL20, GPL20 and MGPL20 gels, the intensities of these bands were clearly stronger indicating changes in the environment around the hydrocarbon side chains.

Thus, the set of results described above contribute to the characterization of two hydrophilic gels, prepared with Poloxamer 407 and Pluronic F-127, by rheology and Raman spectroscopy and assessed the influence of the addition of different actives. The techniques used here are considered non-destructive

and do not interfere in the structure during the procedures involving physical changes [36,37]. The studies on the viscosity and gelation temperature are relevant for the performance of the systems in relation to drug penetration and release in biological system [38,39]. Furthermore, differences due to the presence of cations were observed in systems using copolymers with the same chemical structure, but different molecular weights. The different G' and G'' values obtained for the two PL and PO concentrations in Fig. 1 point to a non-linear behavior for frequencies below 2 Hz. These parameters are characteristic of the stored elastic energy and the viscous dissipated energy, respectively. In most cases, the elastic modulus, G', was greater than the viscous modulus, G'', throughout the frequency range, which is representative of a gel [40]. According to Rao et al., G'' values (loss moduli) higher than G' values (storage moduli) indicate higher dissipation energy applied to deform the system. In this case, the phase differences between the excitation and response was higher and the system has lower damping, indicating liquid phase weak gel-like behavior when the G' value was 10-fold lower than the G'' value [41]. The subsequent decrease in the elastic component corresponded to the unraveling of the network, which resulted in the destruction of the gel [42]. The gels showed a non-Newtonian behavior characterized by a dependence of G' and G'' on the lower values of frequency. They exhibited pseudoplastic behavior with the decreasing viscosity as a function of the shear rate. The increasing G' values in gels prepared with higher polymer concentration exhibited a higher tensile strength because they present a greater elastic component. This finding indicated polymer–polymer and/or polymer–polymer–actives interaction between the components.

The results of the Raman spectroscopy show that the skeletal optical modes within the range 1000–1150 cm^{-1} are particularly sensitive to the conformational state of the hydrocarbon chains. The peak height ratios I_{1065}/I_{1088} and I_{1137}/I_{1088} are commonly used to estimate the relative population of the *trans* and *gauche* conformers [43,44]. The peak 1088 cm^{-1} appears in the GPO20 in agreement with the presence of gadusol in the polymer gel, which, in some way, seems to alter the chains of the polymer to *gauche* conformation. In general, the *gauche* conformations are observed in amorphous segments. The random presence of *gauche* and *trans* bonds is in line with a less structured crystalline arrangement [45]. Complementary information with Raman spectroscopy can be observed in Fig. 1 since G' and G'' values are higher for GPO20 than for MPO20 and MGPO20. Figure 2 shows a lower saturation value as a function of temperature. When $G' < G''$, elastic properties are negligible and the samples can be characterized as viscous rather than as elastic liquids. The opposite behavior was found for the MGPO20 gel, which showed larger areas for peaks at 1068 and 1137 cm^{-1} in addition to viscous behavior (G'') that remained constant in the frequency range explored (Fig. 1) and presented values of G'' lower than for the GPO20 sample. Figure 2 indicates that a higher initial value of the complex viscosity MGPO20 achieved greater apparent viscosity value than the GPO20 sample at the same temperature (26.3°C). A higher value of the apparent viscosity may be related to the fact that the predominant structures are dendritic and not coiled, in the view of the last one incorporating more liquid within the chains [45]. The frequency shift in the bands near 1174 cm^{-1} for the GPO20 samples and the occurrence of the 1180 cm^{-1} mode in the PL20 are related to changes in the C–H bending since these modes are sensitive to environmental conformational changes [26]. In this same sample (GPO20), the 1252 cm^{-1} peak can be related to a change of the O–CH_2–CH_2–O group corresponding to the PEO chain that transforms to a *gauche* conformation [30], whereas all the other samples keep their area and Raman shift values. The lower area for the 1282 cm^{-1} band indicates that the twist of the CH_2 group changes in the presence of gadusol. However, no changes were observed for the other samples. Differences in the effects of the actives can be explained by considering their chemical structures. In fact, the three molecules show high hydrophilic character and, according to their pKa values, are expected to carry ionic charges under the

neutral pH verified in our experiments [14,21]. Gadusol structure shares four OH groups, while any of the MAA keeps only three OH plus two amino acids moieties. Thus, it is expected that the interactions with the hydrophilic portions of the polymers are significant and distinctive for each class of molecules, in terms of their respective capacity of forming H bonds. This in turn may determine the extent of perturbation of the polymer arrangements

The influence of gadusol on the rheology and structural conformations is more evident for PO chains than for PL. This is probably due to the fact that pluronic gels show a greater degree of crosslinking, according to the viscosity observed, thus preventing major alterations.

We assume that the larger areas in the 1410 cm^{-1} band for gels with PL are due to the presence of cations of polymer that attract water molecules. Thus, the surroundings of the chains are less hydrated, this intensifying the OH vibrational modes in the network.

4. Conclusions

Raman spectroscopy and rheology determinations were carried out to study the behavior of block copolymers in gel incorporating natural UV-absorbing and antioxidant actives, mycosporine-like amino acids and gadusol.

The rheology measurements showed differences in the mechanical spectrum in the presence of actives, mostly gadusol. The advantage of using Raman spectroscopy to investigate PEO–PPO–PEO triblock copolymers in neat gels or with actives is evident since several bands in the spectra are sensitive to the structure and conformational changes of the copolymers. The MGPO20 sample presented higher contributions of peaks related to *trans* conformation of the C–C bonds located in the hydrophilic polymer (PEO), whereas GPO20 showed a lower area of the same peaks. Furthermore, the C–C bonds in GPO20 seem to exhibit *gauche* conformation correlating with higher values of G' and G'', according to the complementary rheological information. It is possible that the C–C backbone in the MGPO20 sample reaches higher level of order and more stretched arrangements due to the increasing number of hydrophilic groups in the samples containing both actives.

Acknowledgements

We thank Javier Perez – INTEMA Mar del Plata, Argentina for the rheological measurements. This work was supported by the Consejo Nacional de Investigaciones Científicas y Técnicas – CONICET – Argentina (PIP 112-201001-00211) and SECYT-UBA 2011/2014.

References

[1] Antunes FE, Gentile L, Rossi CO, Tavano L, Ranieri GA. Gels of Pluronic F127 and nonionic surfactants from rheological characterization to controlled drug permeation. Colloids and Surfaces B: Biointerfaces. 2011;87(1):42–8.

[2] Corrêa NM, Camargo FB Jr, Ignácio RF, Leonardi GR. Avaliaçao do comportamento reológico de diferentes géis hidrofílicos. Brazilian J Pharm Sciences. 2005;41(1):73–8.

[3] Moreira TS, Sousa VP, Pierre MBR. Influence of oleic acid on the rheology and in vitro release of lumiracoxib from poloxamer gels. Journal of Pharmacy & Pharmaceutical Sciences. 2010;13(2):286–302.

[4] Escobar-Chávez JJ, Quintanar-Guerrero D, Ganem-Quintanar A. In vivo skin permeation of sodium naproxen formulated in Pluronic F-127 gels: Effect of Azone and Transcutol. Drug Dev Ind Pharm. 2005;31:447–54.

[5] Veyries ML, Couarraze G, Geiger S, Agnely F, Massias L, Kunzli B, et al. Controlled release of vancomycin from Poloxamer 407 gels. Int J Pharm. 1999;192(2):183–93.
[6] Escobar-Chávez JJ, López-Cervantes M, Naik A, Kalia YN, Quintanar-Gerrero D, Ganem-Quintanar A. Applications of thermo-reversible Pluronic F-127 gels in pharmaceutical formulations. Journal of Pharmacy & Pharmaceutical Sciences. 2006;9(3):339–58.
[7] Kaminski GAT, Silverio LC, Pasqualim P, Fin MT, Sasso DGB, Fujiwara GM, et al. Evaluation of oil variability and its influence on hydrophilic low molecular weight drugs microencapsulation by w/o emulsification. Visao Acadêmica. 2010;11(1):45–54.
[8] Djabri A, Guy RH, Delgado-Charro MB. Transdermal iontophoresis of ranitidine: An opportunity in paediatric drug therapy. Int J Pharm. 2012;435(1):27–32.
[9] Singh S, Gajra B, Rawat M, Muthu MS. Enhanced transdermal delivery of ketoprofen from bioadhesive gels. Pakistan Journal of Pharmaceutical Sciences. 2009;22(2):193–8.
[10] Son YJ, Yoo HS. Dexamethasone-incorporated nanofibrous meshes for antiproliferation of smooth muscle cells: Thermally induced drug-loading strategy. Journal of Biomedical Materials Research Part A. 2012;100(10):2678–85.
[11] Chiheb I, Riadi H, Martinez-Lopez J, Dominguez Seglar JF, Vidal JAG, Bouziane H, et al. Screening of antibacterial activity in marine green and brown macroalgae from the coast of Morocco. African Journal of Biotechnology. 2009;8(7):1258–62.
[12] de la Coba F, Aguilera J, de Gálvez MV, Álvarez M, Gallego E, Figueroa FL, et al. Prevention of the ultraviolet effects on clinical and histopathological changes, as well as the heat shock protein-70 expression in mouse skin by topical application of algal UV-absorbing compounds. Journal of Dermatological Science. 2009;55(3):161–9.
[13] de la Coba F, Aguilera J, Figueroa FL, Gálvez MV, Herrera E. Antioxidant activity of mycosporine-like amino acids isolated from three red macroalgae and one marine lichen. Journal of Applied Phycology. 2008;21(2):161–69.
[14] Shick JM, Dunlap WC. Mycosporine-like amino acids and related gadusols: Biosynthesis, accumulation, and UV-protective functions in aquatic organisms. Annual Review of Physiology. 2002;64(1):223–62.
[15] García-Abuín A, Gómez-Díaz D, Navaza JM, Regueiro L, Vidal-Tato I. Viscosimetric behaviour of hyaluronic acid in different aqueous solutions. Carbohydrate Polymers. 2011;85(3):500–5.
[16] Lorenzo G, Zaritzky N, Califano A. Rheological analysis of emulsion-filled gels based on high acyl gellan gum. Food Hydrocolloids. 2013;30(2):672–80.
[17] Farquharson S, Smith W, Rose J, Shaw M. Correlations between molecular (Raman) and macroscopic (rheology) data for process monitoring of thermoset composites. JPAC Process Analytical Chemistry. 2002:45–53.
[18] Liu J, Chen G, Jiang M. Supramolecular hybrid hydrogels from noncovalently functionalized graphene with block copolymers. Macromolecules. 2011;44:7682–91.
[19] Conde FR, Churio MS, Previtali CM. The photoprotector mechanism of mycosporine-like amino acids. Excited-state properties and photostability of porphyra-334 in aqueous solution. Journal of Photochemistry and Photobiology B: Biology. 2000;56(2-3):139–44.
[20] Conde FR, Churio MS, Previtali CM. The deactivation pathways of the excited-states of the mycosporine-like amino acids shinorine and porphyra-334 in aqueous solution. Photochemical & Photobiological Sciences. 2004;3:960–7.
[21] Plack PA, Fraser NW, Grant PT, Middleton C, Mitchell AI, Thomsont RH. Gadusol, an enolic derivative of cyclohexane-1, 3-dione present in the roes of cod and other marine fish. Biochemist Journal. 1981;199:741–7.
[22] Bandaranayake WM, Bourne DJ, Sim RG. Chemical composition during maturing and spawning of the Sponge Dysidea herbacea (Porifera: Demospongiae). Comparative Biochemistry and Physiology Part B: Biochemistry and Molecular Biology. 1997;118(4):851–9.
[23] Arbeloa EM, Uez MJ, Bertolotti SG, Churio MS. Antioxidant activity of gadusol and occurrence in fish roes from Argentine Sea. Food Chemistry. 2010;119(2):586–91.
[24] Schmolka IR. A review of block polymer surfactants. Journal of the American Oil Chemists' Society. 1977;54(3):110–16.
[25] Malmsten M. Soft drug delivery systems. Soft Matter. 2006;2:760–9.
[26] Šturcová A, Schmidt P, Dybal J. Role of hydration and water coordination in micellization of pluronic block copolymers. Journal of Colloid and Interface Science. 2010;352(2):415–23.
[27] Chrit L, Hadjur C, Morel S, Sockalingum G, Lebourdon G, Leroy F, et al. In vivo chemical investigation of human skin using a confocal Raman fiber optic microprobe. Journal of Biomedical Optics. 2005;10(4):44007.
[28] Brookes A, Dyke JM, Hendra PJ, Meehan S. The FT-Raman spectroscopic study of polymers at temperatures in excess of 200°C. Spectrochimica Acta Part A. 1997;53:2313–21.
[29] Fukuhara K, Sagawa T, Kihara S, Matsuura H. Extended oxyethylene chain in triblock compounds al-octyl-w-octyloxyoligo (oxyethylene)s studied by Raman spectroscopy. Journal of Molecular Structure. 1996;379:197–204.
[30] O'Faolaion E, Hunter M, Byrne J, Kellehan P, McNamara M. A study examining the effects of tissue processing on human tissue sections using vibrational spectroscopy. Materials synthesis and applications. Dublin Institute of Technology. 2005.

[31] Edwards HGM, Garcia-Pichel F, Newton EM, Wynn-Williams DD. Vibrational Raman spectroscopic study of scytonemin, the UV-protective cyanobacterial pigment. Spectrochimica Acta Part A, Molecular and Biomolecular Spectroscopy. 2000;56(1):193–200.
[32] Gunasekaran S, Sailatha E, Seshadri S, Kumaresan S. FTIR, FT Raman spectra and molecular structural confirmation of isoniazid. Indian Journal of Pure & Applied Physics. 2009;47(January):12–8.
[33] Guo C, Liu H, Wang J, Chen J. Conformational structure of triblock copolymers by FT-Raman and FTIR spectroscopy. Journal of Colloid and Interface Science. 1999;209(2):368–73.
[34] Larkin P. Correlations: Characteristic group frequencies. San Diego, USA: Elsevier; 2011. p. 73–115.
[35] Movasaghi Z, Rehman S, Rehman IU. Raman spectroscopy of biological tissues. Applied Spectroscopy Reviews. 2007;42(5):493–541.
[36] Winter HH, Mours M. Advances in polymer science. Dusek K, editor. Amherst, USA: Springer; 1997. p. 165–234.
[37] Alvarez-Román R, Naik A, Kalia YN, Guy RH, Fessi H. Skin penetration and distribution of polymeric nanoparticles. Journal of Controlled Release. 2004;99(1):53–62.
[38] Wang J-Y, Marks J, Lee KYC. Nature of interactions between PEO–PPO–PEO triblock copolymers and lipid membranes: (I) effect of polymer hydrophobicity on its ability to protect liposomes from peroxidation. Biomacromolecules. 2012;13(9):2624–33.
[39] Steffe JF. Rheological methods in food process engineering. 2nd ed. East Lansing, MI: Freeman Press; 1996. Chapter 5, Viscoelasticity; p. 294–349.
[40] Rao MA. Rheology of fluid and semisolid foods: Principles and applications. 2nd ed. Geneva, NY, USA: Springer; 2007.
[41] Hsu S, Lu S, Huang C. Viscoelastic changes of rice starch suspensions during gelatinization. JFS: Food Chemistry and Toxicology. 2000;65(2):215–20.
[42] Lee DC, Chapman D. Infrared spectroscopic studies of biomembranes and model membranes. Bioscience Reports. 1986;6(3):235–56.
[43] Wong PTT, Murphy WF, Mantsch HH. Pressure effects on the Raman spectra of phospholipid membranes: Pressure induced phase transitions and structural changes in 1,2-dimyristoyl 3-sn-phosphatidylcholine water dispersions. The Journal of Chemical Physics. 1982;76(11):5230.
[44] Chai CK, Dixon NM, Gerrard DL, Reed W. Rheo–Raman studies of polyethylene melts. Polymer. 1995;36(3):661–3.
[45] Maria do Carmo BV. Caracterizaçao da viscosidade aparente no estado semi-sólido e das propriedades mecanicas da liga AA7075. 2003. Available from: http://hdl.handle.net/10183/7894.
[46] Guo C, Wang J, Liu H-z, Chen J-y. Hydration and conformation of temperature-dependent micellization of PEO–PPO–PEO block copolymers in aqueous solutions by FT-Raman. Langmuir. 1999;15(22):2703–8.